View Article Online
View Journal

Catalysis Science & Technology

Accepted Manuscript

This article can be cited before page numbers have been issued, to do this please use: P. T. Gomes, T. C. Cruz, L. C. J. Pereira, J. C. Waerenborgh and L. F. Veiros, *Catal. Sci. Technol.*, 2019, DOI: 10.1039/C8CY02319K.

This is an Accepted Manuscript, which has been through the Royal Society of Chemistry peer review process and has been accepted for publication.

Accepted Manuscripts are published online shortly after acceptance, before technical editing, formatting and proof reading. Using this free service, authors can make their results available to the community, in citable form, before we publish the edited article. We will replace this Accepted Manuscript with the edited and formatted Advance Article as soon as it is available.

You can find more information about Accepted Manuscripts in the author guidelines.

Please note that technical editing may introduce minor changes to the text and/or graphics, which may alter content. The journal's standard Terms & Conditions and the ethical guidelines, outlined in our author and reviewer resource centre, still apply. In no event shall the Royal Society of Chemistry be held responsible for any errors or omissions in this Accepted Manuscript or any consequences arising from the use of any information it contains.

ROYAL SOCIETY OF CHEMISTRY

rsc.li/catalysis

Hydroboration of terminal olefins with pinacolborane catalyzed by new 2-iminopyrrolyl iron(II) complexes

Tiago F. C. Cruz,[a] Laura C. J. Pereira,[b] João C. Waerenborgh,[b] Luís F. Veiros[a] and Pedro T. Gomes*[a]

[a] *Centro de Química Estrutural, Departamento de Engenharia Química, Instituto Superior Técnico, Universidade de Lisboa, Av. Rovisco Pais 1, 1049-001 Lisboa, Portugal.*

[b] *C²TN-Centro de Ciências e Tecnologias Nucleares, Instituto Superior Técnico, Universidade de Lisboa, 2695-066 Bobadela LRS, Portugal.*

ABSTRACT: Four paramagnetic 14-electron tetracoordinated Fe(II) complexes of 5-substituted-2-iminopyrrolyl ligands of the type [Fe{κ²*N,N'*-5-R-NC_4H_2-2-C(H)=N(2,6-$^iPr_2$-C_6H_3)}(Py)Cl], with R = 2,6-Me_2-C_6H_3 (**1a**), 2,4,6-$^iPr_3$-C_6H_2 (**1b**), 2,4,6-Ph_3-C_6H_3 (**1c**) and CPh_3 (**1d**), were synthesized in moderate yields by reacting the respective 5-substituted-2-iminopyrrolyl potassium salts **KLa-d** with $FeCl_2(Py)_4$ in toluene. Complexes **1a-d** were characterized by ^{1}H NMR and FTIR spectroscopies, elemental analysis, and by the Evans method, the corresponding effective magnetic moments showing a high-spin electronic nature. X-ray diffraction studies on complexes **1a** and **1c** showed distorted tetrahedral coordination geometries. Complexes **1a-c**, activated with K($HBEt_3$), were efficient catalyst systems for the hydroboration of several terminal alkenes with pinacolborane in good to high yields (50-90 %). This system mainly yielded the respective *anti*-Markovnikov addition products, except when styrenes were used. A screening of the hydroboration of styrene catalyzed by complexes **1a-c** activated with K($HBEt_3$) showed that the selectivity in the Markovnikov product increased with increasing steric bulkiness of the R group, exhibiting selectivities up to 91%. Additionally, the stoichiometric reaction of complex **1b** with K($HBEt_3$) over 30 minutes yielded the mixture of hydride species **2** and $\mathbf{2_2}$ (mixture I). On the other hand, when reacting the same components over 16 h, the Fe(I) complex **3** was also identified in the mixture, in addition to **2** + $\mathbf{2_2}$ (mixture II). These mixtures were characterized in solution by the Evans method and in the solid state by elemental analysis, ^{57}Fe Mössbauer and FTIR spectroscopies, compounds $\mathbf{2_2}$ and **3** being also analyzed by X-ray diffraction. These results suggest that the corresponding catalytic cycle follows the borane oxidative addition route to a Fe(I) species.

View Article Online
DOI: 10.1039/C8CY02319K

Keywords: 2-iminopyrrolyl ligands; tetracoordinated iron(II) complexes; hydroboration of terminal alkenes; iron(II) hydride complexes; iron(I) arene complexes.

View Article Online
DOI: 10.1039/C8CY02319K

Introduction

The use of organoboron compounds in organic synthesis paves the way to carbon-heteroatom bond formation, for example via stereospecific cross-coupling or oxidation reactions, making them an important class of reagents.[1] An important source of organoboranes is the hydroboration of alkenes, which has often been catalyzed by platinum group elements, such as rhodium or iridium.[2] The need for metal-catalyzed hydroboration is justified as it allows the use of rather unreactive boranes, such as pinacolborane (HBPin), which are often more selective in subsequent organic synthetic steps. The expensive and rather toxic characteristics of the Rh or Ir elements have led researchers to develop alternative cheap and abundant mediators.[3] For these reasons, iron and cobalt have been increasingly used as metals in catalytic alkene hydroboration reactions.[4]

As far as utilizing iron as the metal in complexes capable of catalyzing hydroboration of alkenes with HBPin is concerned, some works are to be noted. Chirik and co-workers developed and used [bis(imino)pyridine]Fe$(N_2)_2$ or [bis(imino)pyridine]$FeCl_2$ complexes (**A**, Chart 1), the latter activated by Na$(HBEt_3)$, in the hydroboration of alkenes with HBPin.[4a] Iron complexes using monoanionic ligands have also been explored in hydroboration reactions. Szymczak *et al.*, used a *N,N,N* tridentate [1,3-bis(6'-methyl-2'-pyridylimino)isoindolate]FeBr for hydroboration regulated by an outer-sphere effect, activated by K$(HBEt_3)$.[4k] Also, a *P,N* bidentate complex (*N*-phosphinoamidinate)Fe[N$(SiMe_3)_2$] (**B**, Chart 1), reported by Turculet *et al.*, catalyzed hydroborations in neat and mild conditions.[4e] All the examples mentioned above led to an *anti*-Markovnikov selectivity of the addition products.

In contrast, Thomas *et al.* used an alkoxy-tethered *N*-heterocyclic carbene Fe(II) complex (**C**, Chart 1) that proved to be Markovnikov-selective towards the hydroboration of alkenes.[4g] In a similar approach, Webster and co-workers reiterated the importance of ligand design in the selectivity of hydroboration products, using LFe(CH_2SiMe_3) complexes (**D**, Chart 1), with L being a β-diketiminate ligand of varying stereochemical bulkiness.[4j]

View Article Online
DOI: 10.1039/C8CY02319K

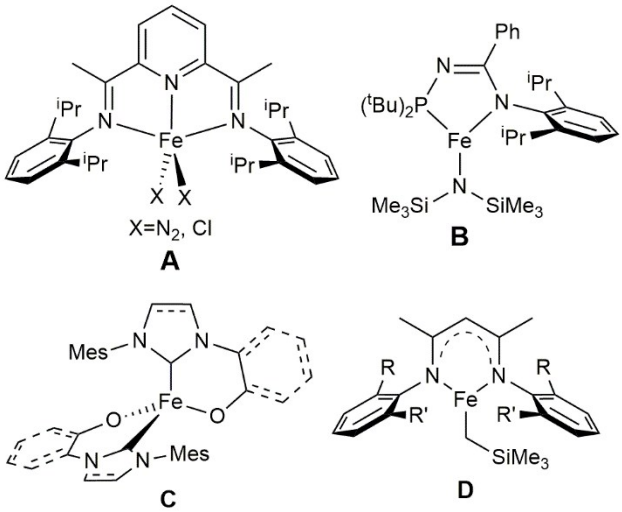

Chart 1 Iron complexes used in the hydroboration of terminal alkenes.

The coordination chemistry of Fe with a single monoanionic bidentate *N,N* ligand bearing a chloride co-ligand is not extensively explored. The *N,N* β-diketiminate ligand system has allowed for the successful preparation of complexes of the type L^1FeCl and $L^2Fe(\mu\text{-}Cl)_2Li(THF)_2$, or $[L^3FeX]_2$, with X=Cl or Br, with L being bulky β-diketiminate ligands (**A**, Chart 2), reported by Holland *et al.*[5] With a different system, the complexes of the type $[LFeCl]_2$, with L being a bulky amidinate ligand (**B**, Chart 2), were prepared by Jones *et. al.*[6] Betley and co-workers also synthesized complexes of the type LFeClPy bearing dipyrromethane ligand derivatives (**C**, Chart 2).[7]

The chemistry of iron bearing the 2-iminopyrrolyl system is very limited and only involves the inclusion of two ligands of that type. The first reported case was the bis[2-*N*-(arylimino)pyrrolyl] iron complex, FeL_2, with L being 2,6-bis(imino)pyrrolyl ligands with only one of the imine arms coordinated to Fe (**D** ,Chart 2), by Bochmann and co-workers.[8] Sun *et al.* also reported the $FeL_2(PMe_3)_2$ complexes, with L being a 2-benzyliminopyrrolyl ligand, via a NH bond activation reaction with $Fe(PMe_3)_4$.[9] Lately, we have been interested in the coordination chemistry of complexes bearing 2-iminopyrrolyl ligands, having prepared compounds of the late-transition metals Co,[10] Ni and Cu[11] and Zn,[12] all having at least two 2-iminopyrrolyl or 2-iminophenanthropyrrolyl ligands. We have also prepared Na[13] and B[14] compounds of these ligands and have been able to crystalographically characterize the Fe(III) oxo complexes bearing two 2-iminopyrrolyl ligands, highlighting the high sensitivity to air and moisture of the putative $Fe[2\text{-iminopyrrolyl}]_2$. However, we managed to stabilize that fragment with the addition of a pyridine (Py) ligand (**E**, Chart 2).[11]

View Article Online
DOI: 10.1039/C8CY02319K

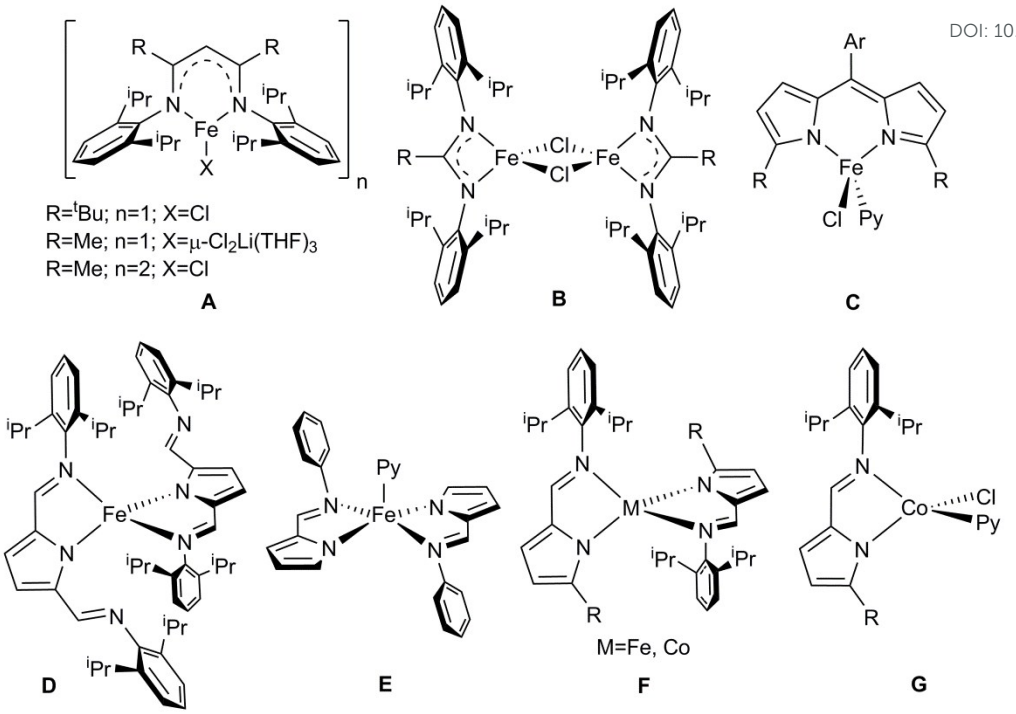

Chart 2 Low-coordinate iron(II) halide complexes (**A**–**C**) and 2-iminopyrrolyl iron(II) (**D**–**F**) and cobalt(II) (**F**, **G**) complexes.

Our group has recently reported the preparation of bulky 5-substituted-2-iminopyrrole ligand precursors, from their corresponding 5-substituted-2-formylpyrroles,[15] and subsequently used them to prepare homoleptic [M(5-substituted-2-iminopyrrolyl)$_2$] complexes of Fe(II) and Co(II) (**F**, Chart 2).[16] In a subsequent work, we were able to avoid the synthesis of bis chelates and prepared a family of mono(5-substituted-2-iminopyrrolyl) Co(II) complexes (**G**, Chart 2), which proved to be active in the hydroboration of terminal alkenes upon activation by K(HBEt$_3$),[17] as well as aryl Ni(II) complexes containing a single 5-substituted-2-iminopyrrolyl ligand that are active in the production of hyperbranched polyethylene.[18] Taking these results into account, we now present the extension of the coordination chemistry of the bulky 5-substituted-2-iminopyrrolyl ligands to iron, and the application of these new mono(2-iminopyrrolyl) complexes as efficient precatalysts for the hydroboration of terminal alkenes with HBPin.

Results and discussion

Synthesis and characterization of the pyridine chloride iron(II) precatalysts: The Fe(II) complexes of the type [Fe{κ^2*N,N'*-5-R-NC$_4$H$_2$-2-C(H)=N(2,6-^{i}Pr$_2$-C$_6$H$_3$)}(Py)Cl] (**1a-d**) were prepared in moderate yields by the metathetic salt reaction of FeCl$_2$(Py)$_4$ with the respective

View Article Online
DOI: 10.1039/C8CY02319K

potassium salts **KLa-d**[17] in toluene, at 80 ºC (Scheme 1). Complexes **1a-d** were isolated as orange-red powders or crystals from concentrated toluene/*n*-hexane solutions after standard work-up procedures.

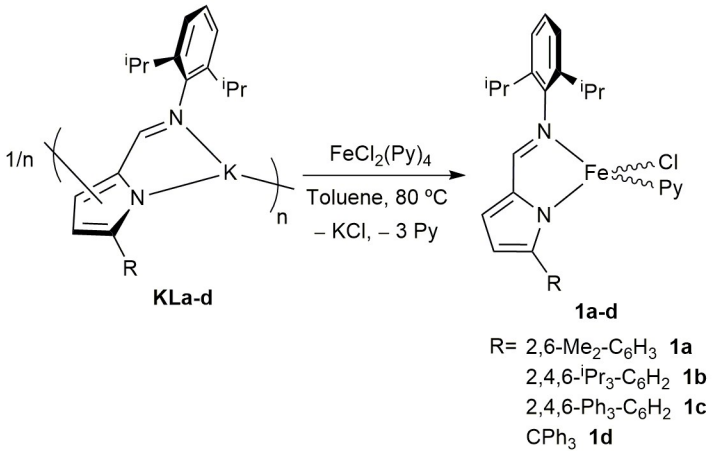

Scheme 1 Synthesis of the pyridine chloride iron(II) complexes **1a-d**.

All complexes are paramagnetic and are very sensitive to air and moisture both in solution and in solid state, since they are highly unsaturated 14-electron species, with two potentially labile cis coordination sites. These complexes are partially soluble in *n*-hexane and Et_2O and soluble in toluene. Preliminary synthesis attempts of chloride Fe(II) complexes of this ligand system were made by reacting the referred potassium salts with $FeCl_2$ in THF. This pathway, however, was marred by very troublesome purification procedures and unexpected decomposition of the reaction intermediates. The respective combustion analyses of these reactions proved to be inconclusive, pointing to adducts of the mono chelated chloride complexes with KCl and THF.

Complexes **1a-d** were characterized in solution by ^{1}H NMR spectroscopy, their respective spectra being shown in Figures S1-S4 of the ESI. Complexes **1a-d** display paramagnetically shifted ^{1}H NMR spectra, which resonances can tentatively be assigned to their respective 5-substituted-2-iminopyrrolyl chelates and to the pyridine ligand.

In toluene-d_8 solutions, complexes **1a-d** showed effective magnetic moments (measured by the Evans method[19]) in the range of 4.6-5.3 μ_B (see Table 1), which is characteristic of a d^6 metal ion in the high-spin state (S = 2; μ_{eff} (spin-only) = 4.9 μ_B) with some degree of spin-orbit coupling effects.[20] Further studies in the solid state were performed on complex **1a** by SQUID magnetometry (see Figure S14 of the ESI). As expected for a tetracoordinated Fe(II)

View Article Online
DOI: 10.1039/C8CY02319K

complex, this compound is paramagnetic, with $S = 2$. At room temperature, $\mu_{eff} = 4.86\ \mu_B$, in good agreement with the value obtained in solution.

Table 1 Effective magnetic moments μ_{eff} (μ_B) for the Fe(II) complexes **1a-d**, measured in toluene-d_8 solution (Evans method), at room temperature.

Complex	μ_{eff} (μ_B)
1a	5.3
1b	4.8
1c	4.6
1d	4.7

Complexes **1a-d** were characterized by FTIR spectroscopy, the respective spectra being shown in Figures S7-S10 of the ESI. As expected, the spectra of the four complexes are very similar, being possible to observe the typically sharp C=N bond stretching vibration bands, at 1561-1573 cm^{-1}.

Complexes **1a** and **1c** were also characterized in the solid state by X-ray diffraction. Crystals of **1a** and **1c** were obtained from a toluene:*n*-hexane solution (1:3 in volume) cooled to -20 ºC, and crystalized in the monoclinic system in the $P2_1$ and $P2_1/c$ space groups, respectively. The structure of complex **1a** is shown in Figure 1, with selected bond lengths and angles being listed in Table S1 of the ESI. The structure of complex **1c**, owing to the poor quality of its diffraction data, is only shown in the ESI (Figure S13 and Table S1) as additional structural evidence.

In complex **1a**, it is possible to observe that a single 5-aryl-2-iminopyrrolyl ligand is coordinated to the metal center in a bidentate fashion through the pyrrolyl (N1) and iminic (N2) nitrogen atoms in a near planar five-membered chelate (Fe1−N1−C2−C6−N2). The tetracoordinated metal centers are further bonded to a chlorine atom and a pyridine ligand. The Fe−N bond lengths are in the range of 2.0308(19)−2.112(2) Å, in the order Fe1−N1<Fe1−N3<Fe1−N2, very likely associated with the decreasing degree of the σ character of the respective bonds. The Fe1−N bond lengths are longer than in the analogous Co(II) complexes [Co{κ^2*N,N'*-5-R-NC_4H_2-2-C(H)=N(2,6-^{i}Pr_2-C_6H_3)}(Py)Cl] (R=2,6-Me_2-C_6H_3 or 2,4,6-Ph_3-C_6H_2) reported by our group,[17] attributed to the lower electronegativity (higher ionic radius) of the Fe(II) center. The τ_4 parameter for complex **1a** is 0.74 ($\tau_4 = 0$ for an ideal square planar geometry and $\tau_4 = 1$ for an ideal tetrahedral geometry[21]), thus corresponding to a distorted tetrahedral geometry.

View Article Online
DOI: 10.1039/C8CY02319K

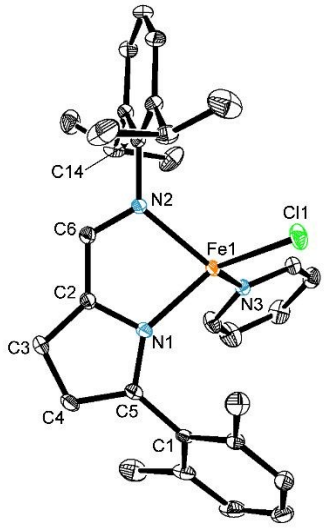

Figure 1 ORTEP-3 diagram for complex **1a** showing 30% probability ellipsoids. All hydrogen atoms were omitted for clarity.

The molecular structure of the complexes presented above was probed by DFT calculations.[22] Geometry optimizations were performed for the family of complexes **1a-d** in the high spin electronic state, $S = 2$. The atomic coordinates of all optimized complexes are presented in the ESI. All complexes exhibit a distorted tetrahedral geometry and their τ_4 parameters are in the range 0.73−0.77, comparing well with the experimentally determined structures of complexes **1a** and **1c**. The calculated Fe-N bond lengths lie in the range 2.025−2.184 Å and in the order Fe−N1<Fe−N3<Fe−N2. On the other hand, the Fe−Cl bond lengths are in the range 2.241−2.260 Å, being almost invariant with the 5-substituent. When comparing the calculated bond lengths with the ones determined by X-ray diffraction (in complexes **1a** and **1c**) one can see a maximum absolute deviation of 0.08 Å. These results are in good agreement and reinforce that the experimentally determined high-spin electronic configurations are corroborated by DFT calculations.

Complex **1a** was also characterized by Mössbauer spectroscopy. The Mössbauer spectra taken at 4 and 295 K (Figure S15 of the ESI) consist of symmetric two-peak patterns, which are fitted with single quadrupole doublets in agreement with a single crystallographic site for Fe in **1a**. The estimated isomer shifts, IS = 0.88 mm s^{-1} at 4 K and 0.77 mm s^{-1} at 295 K (Table S5 of the ESI), are consistent with high-spin Fe(II) ($S = 2$).[23,24] The increase of IS with increasing temperature is explained by the second order Doppler shift. The quadrupole splitting values (QS = 2.41 mm/s at 4 K and 2.16 mm/s at 295 K) as well as their temperature dependence are also typical of high-spin Fe(II).

View Article Online
DOI: 10.1039/C8CY02319K

Catalytic hydroboration studies: The coordinative and electronic unsaturation of the Fe(II) complexes **1a-d** showed that they are good candidates to precatalysts for hydrofunctionalization reactions. We were also driven by the encouraging results obtained in the hydroboration of terminal alkenes with pinacolborane (HBPin) precatalyzed by our analogous Co(II) complexes, activated by K(HBEt$_3$).[17] Firstly, we analyzed the α-olefin scope with the **1a**/K(HBEt$_3$) catalytic system. The results for the substrate scope study with the **1a**/K(HBEt$_3$) system are presented in Table 2 and the ^{1}H NMR spectra of the alkylboronate products are shown in Figures S16-S26 of the ESI. The system is hydroboration inactive either in the absence of activation by K(HBEt$_3$) or in the absence of complexes **1a-d**.

Table 2 Substrate scope of the hydroboration of terminal alkenes catalyzed by the system **1a**/K(HBEt$_3$).

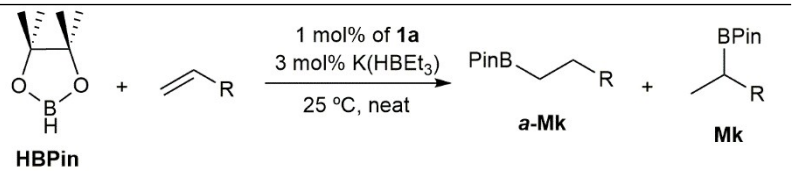

Substrate[a]	Yield (%)[b]	Selectivity (*a*-Mk:Mk)[c]
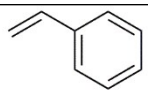	92	0.39:1
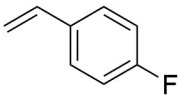	54	0.36:1
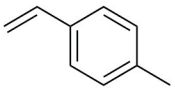	54	0.38:1
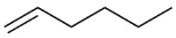	58	2.23:1
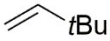	59	1.32:1
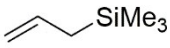	51	2.13:1
	36	-

[a] Conditions: 1 mol% of 1a, 3 mol% of K(HBEt$_3$), 2 mmol of substrate, 2.5 mmol of HBPin, reaction time: 16 h, temperature: 25 ºC. [b] Yields determined by weighing the isolated reaction products. [c] Calculated by ^{1}H NMR.

It is possible to see that the **1a**/K(HBEt$_3$) catalyst system gives rise to a mixture of *anti*-Markovnikov/Markovnikov addition products of the respective terminal alkenes (*a*-Mk/Mk) in good yields (51-92%), under neat and mild conditions. No isomerization was observed in

View Article Online
DOI: 10.1039/C8CY02319K

allylic olefins such as 1-hexene or allyltrimethylsilane. This catalyst system also hydroborates cyclohexene in moderate yield.

It is also notably observed that by screening styrenes *para*-substituted with electronically differentiated groups (1-fluoro-4-vinylbenzene, 1-methyl-4-vinylbenzene) in the same hydroboration reaction, the regioselectivity remains unaltered. Additionally, the present catalyst system was tested with the sterically hindered 1,3,5-trimethyl-2-vinylbenzene, revealing very low conversion (9%) and selectivity towards hydroboration, other uncharacterized products being present after work-up of the catalytic reaction (see Figures S19 of the ESI), being though possible to detect a *a*-Mk/Mk ratio of 0.35:1. Therefore, the styrene substrate scope shows that this catalyst system is sensitive to stereochemical constraints but seems to be independent of electronic variations in the substrate, the hydroboration regioselectivity depending solely on the bulkiness of the chelating ligand of the precatalyst used.

In general, from the substrate scope analysis, it is clear that this system has the tendency to systematically generate a notable amount of the Mk addition product, a fact that was not observed in our Co(II) system, which always showed exclusive *a*-Mk selectivity.[17] However, in this mixture of *a*-Mk and Mk addition products, the **1a**/K($HBEt_3$) system mainly produces the *a*-Mk one, except in the case of styrene, in which the selectivity is reversed, the major isomer produced being the Mk addition product.

As far as styrene is concerned, a major selectivity in the Mk addition product was observed. Therefore, similarly to our Co(II) system, we evaluated the effect of the different precatalysts **1a-d** in the hydroboration of styrene. The results for the hydroboration of styrene with HBPin using the different Fe(II) precatalysts **1a-d** activated by K($HBEt_3$) are shown in Table 3. Also, a superimposition of the ^{1}H NMR spectra of the α-protons relative to the boron atom of the products of the hydroboration of styrene catalyzed by **1a-d**/K($HBEt_3$) is shown in Figure S27 of the ESI.

The Fe(II) pre-catalysts **1a-d** activated by K($HBEt_3$) yielded mixtures of products in moderate to good yields, where the Mk product is systematically the major isomer. It can be concluded that by increasing the steric bulkiness of the *ortho* groups of the 5-aryl substituent, going from methyl (in complex **1a**), to isopropyl (in complex **1b**) to phenyl (in complex **1c**), the system increases the selectivity in the Markovnikov product. In fact, precatalyst **1c** gave rise to a 91% selectivity in the Mk product. Complex **1d** did give rise to a 0.15:1 *a*-MK:Mk ratio of addition products of styrene. However, catalysis by this latter complex was not

View Article Online
DOI: 10.1039/C8CY02319K

completely selective in the hydroboration of styrene, yielding a complex mixture of products (the ^{1}H NMR spectrum of the isolated products is presented in Figure S22 of the ESI).

The yields in the organoboranes produced in this work are in the range of those obtained by other authors that reported iron-catalyzed hydroboration of the same substrates,[4e,g,j,k,l] but can only be considered as moderate when compared with the best results reported to date. In fact, some authors reported yields as high as 98 % for some of the substrates presented in this work, in less than an hour, in similar reaction conditions.[4a,m]

Table 3 Structure/selectivity relationship for the hydroboration of styrene catalyzed by the system **1a-d**/K(HBEt$_3$).

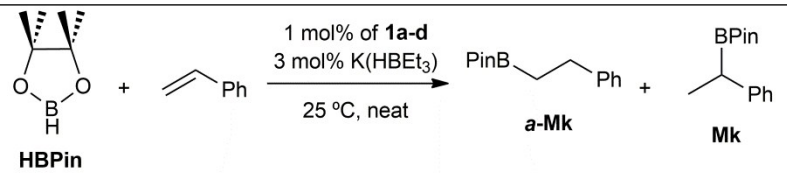

Complex[a]	Yield (%)[b]	Selectivity (*a*-Mk:Mk)[c]
1a	92	0.39:1
1b	92	0.32:1
1c	51	0.09:1
1d	31[d]	0.15:1[d]

[a] Conditions: 1 mol% of **1a-d** 3 mol% of K(HBEt$_3$), 2 mmol of styrene, 2.5 mmol of HBPin, reaction time: 16 h, temperature: 25 ºC. [b] Yields determined by weighing the isolated reaction products. [c] Calculated by ^{1}H NMR. [d] The yield obtained with complex **1d** corresponds to the mixture of addition products presented above, but was not completely selective towards the hydroboration of styrene, as other unidentified products were observed.

The most common selectivity found in the literature for iron-catalyzed hydroboration of alkenes is *anti*-Markovnikov, with several examples showing total selectivity in this type of products.[4a,e,k,m] By contrast, we systematically observed a mixture of addition products, yielding nearly Markovnikov-exclusive products by using precatalyst **1c**. Markovnikov selectivity in iron-catalyzed hydroboration of alkenes is not common and, to date, only few cases have been reported, with *a*-MK:Mk ratios as low as 0.02:1.[4g,j,l]

Stoichiometric reactions of precatalysts 1a-d with K(HBEt$_3$) and mechanistic insights: To understand the mode of activation of the Fe(II) pyridine chloride complexes, we explored their stoichiometric reactivity with the super hydride K(HBEt$_3$). After several attempts, the only reaction that produced isolable materials was the one involving complex **1b**. In fact, the reaction of complex **1b** with one equivalent of K(HBEt$_3$) for 30 minutes, in toluene, led, after

View Article Online
DOI: 10.1039/C8CY02319K

a standard work-up procedure, to the formation of a dark red-brown crystalline solid identified as a mixture of Fe hydride complexes, the monomer **2** and the dimer $\mathbf{2_2}$, with concomitant formation of KCl, BEt_3 and pyridine (Scheme 2, mixture I). This mixture of hydride complexes was characterized by elemental analysis, measurement of magnetic susceptibility in solution (by the Evans method[19]), and by FTIR and Mössbauer spectroscopies. This observation proved slightly puzzling at first, since it contradicted the results previously reported by our group with cobalt, in which the same reaction conditions cleanly led to the formation of the η^6-toluene Co(I) complex [Co{κ^2*N,N'*-5-(2,4,6-^{i}Pr$_3$-C$_6$H$_2$)-NC$_4$H$_2$-2-C(H)=N(2,6-^{i}Pr$_2$-C$_6$H$_3$)}(η^6-C$_6$H$_5$CH$_3$)].[25]

In light of these results, we attempted to obtain the analogous Fe(I) arene complex by further forcing the reaction conditions, using a reaction time of 16 hours. This time around, we were indeed able to identify the reduced complex [Fe{κ^2*N,N'*-5-(2,4,6-^{i}Pr$_3$-C$_6$H$_2$)-NC$_4$H$_2$-2-C(H)=N(2,6-^{i}Pr$_2$-C$_6$H$_3$)}(η^6-C$_6$H$_5$CH$_3$)] (**3**), albeit only corresponding to 10% of the isolated mixture, the remainder 90% still corresponding to the mixture **2** + $\mathbf{2_2}$ (Scheme 2, mixture II). Mixture II of complexes was characterized by elemental analysis, by the Evans method,[19] and by FTIR and Mössbauer spectroscopies. Attempts to isolate analytically pure samples of complex **3** were made through more rational synthetic procedures. Unfortunately, chemical reduction reactions of complex **1b** with Na(Hg) or with KC_8 in toluene only led to decomposition of the reaction mixtures, contrasting with the clean generation of the analogous η^6-toluene Co(I) complex reported previously by our group.[25]

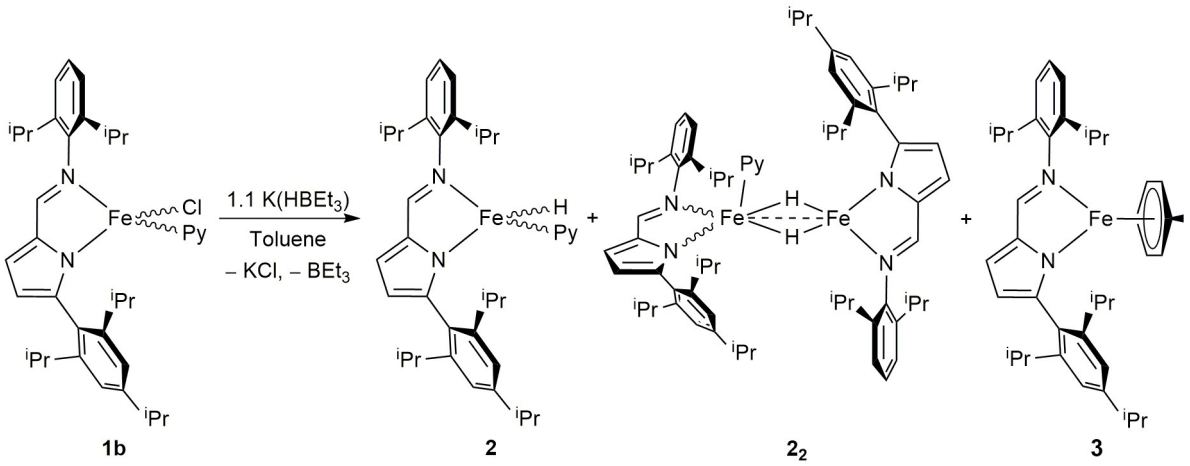

Product ratios (%):			
Reaction time: 30 min (mixture I)	***35***	***65***	***0***
Reaction time: 16 h (mixture II)	***34***	***56***	***10***

Scheme 2 Reaction of complex **1b** with K(HBEt$_3$) at different reaction times, leading,to mixtures I (complexes **2** + $\mathbf{2_2}$) and II (complexes **2** + $\mathbf{2_2}$ + **3**).

View Article Online
DOI: 10.1039/C8CY02319K

Mixtures I and II are very soluble in *n*-hexane and very sensitive to air and moisture, both in solution and in the solid state, readily decomposing with effervescence in protic solvents. These mixtures are of impossible separation, owing to similar solubilities of their respective components. A similar reactivity seems to be observed when the Fe complexes **1a** or **1c** were used as precursors, but the lack of crystallinity of the samples frustrated any X-ray diffraction studies or suitable combustion analyses, preventing an analogous report.

Mössbauer spectroscopy proved instrumental in the qualitative and quantitative characterization of mixtures I and II. The Mössbauer spectra of mixtures I (complexes **2** + $\mathbf{2_2}$) and II (complexes **2** + $\mathbf{2_2}$ + **3**) taken between 4 and 150 K are presented in Figure 3 and may only be adequately fitted if three (for mixture I, Figure 3a) or four (for mixture II, Figure 3b) doublets are refined.

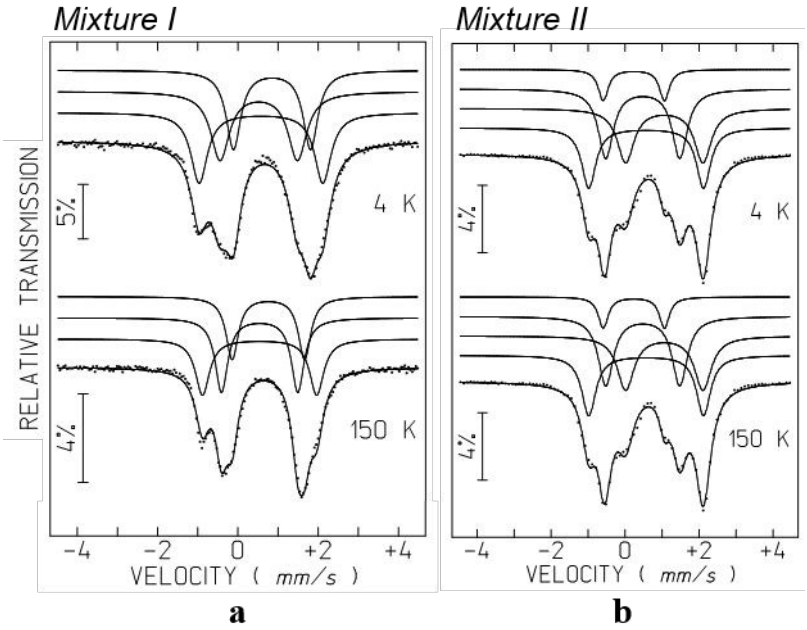

Figure 2 Mössbauer spectra of mixture I (a) and of mixture II (b) taken at different temperatures. Lines above the experimental points are the sum of three (for mixture I) or four (for mixture II) doublets (see also Table S3 of the ESI), shown slightly shifted for clarity.

In mixture I, considering that two molecular entities, a monomeric compound **2**, bearing a terminal hydride ligand, and a dimeric compound $\mathbf{2_2}$, containing μ-bridging hydrides, are present in the sample, one of the doublets may be attributed to the complex that has only one crystallographic site for Fe (**2**, terminal hydride), and the remaining two doublets, with the same relative areas within experimental error (Table S3, shown in the ESI), are assigned to

both crystallographic positions in the dimer (**2₂**, bridging hydrides). The relative area of the doublet attributed to compound **2** corresponds to 35%, and the sum of the relative areas corresponding to **2₂** is 65% (Table S3 of the ESI). This molar composition of the mixture **2**+**2₂**, retrieved from the Mössbauer spectrum at 4 K, perfectly matches the values obtained for the elemental analysis of the sample (within the experimental error), taking into account that **2** really has the formulation suggested in Scheme 2. In fact, in the mixture $(C_{37}H_{49}FeN_3)_{0.35}(C_{69}H_{93}Fe_2N_5)_{0.65}$, the combustion analysis values obtained and calculated (the latter between parentheses) are: C 75.12 (75.07), H 8.50 (8.46), N 6.45 (6.51). The estimated IS values are too large or too low for low-spin or high-spin monovalent Fe, respectively.[23] They are close to the low end of the isomer shifts range of high-spin Fe(II).[23] These low values are usually found for Fe(II) complexes with at least one hydride as a ligand due to the better σ-donating ability of the hydride as compared to the other organic ligands.[26] The temperature dependence of the quadrupole splittings is also consistent with high-spin Fe(II).[23] The lowest measured IS values are due to tetracoordinated Fe(II) in the terminal hydride Fe complex **2** and in the μ-bridging hydrides di-iron complex **2₂** and the highest IS to pentacoordinated Fe(II) in dimer **2₂**, in agreement with the estimated relative areas.

On the other hand, the Mössbauer spectra of mixture II are somewhat different from those of mixture I taken at the same temperatures. These differences are accounted for, in addition to the doublets assigned to the monomeric compound **2**, bearing a terminal hydride ligand, and the dimeric compound **2₂**, containing μ-bridging hydrides, the appearance of a fourth doublet, corresponding to a 10 % molar contribution to the mixture, at 4 K. The estimated IS values for this doublet at 4 K and 150 K (Table S3, shown in the ESI) are within the range of IS values that have been reported in the literature for high-spin Fe(I) complexes (S = 3/2).[27] In addition, as observed for mixture I, the combustion analysis values of mixture B are in accordance with the molar ratios determined by Mössbauer spectroscopy, the obtained and calculated (the latter between parentheses) values for the entity $(C_{37}H_{49}FeN_3)_{0.34}(C_{69}H_{93}Fe_2N_5)_{0.56}(C_{39}H_{51}FeN_2)_{0.1}(\text{-OSi}(CH_3)_2\text{-})_{0.5}$, being C 72.93 (73.48), H 8.47 (8.45), N 6.05 (6.14).

The FTIR spectra of mixtures I and II are presented in Figures S11 and S12, respectively, being nearly superimposable. The C=N stretching bands of the mixtures are present at 1565 cm^{-1}, irrespective of the observed mixtures of complexes. Despite the apparent low sensitivity of this technique towards C=N bond stretching vibrations in these mixtures, the FTIR spectrum of mixture II clearly displays three bands at 799, 788 and 776 cm^{-1}, which were not

View Article Online
DOI: 10.1039/C8CY02319K

observed in the FT-IR spectrum of mixture I, being diagnostic of the additional toluene moiety of complex **3** present in mixture II.

Complexes $\mathbf{2_2}$ and **3** were further characterized by X-ray diffraction, having crystallized in the triclinic system, in the P-1 space group. The molecular structures of complexes $\mathbf{2_2}$ and **3** are shown in Figure 2, with selected bond lengths and angles being presented in Tables S2 and S3 of the ESI. Complex $\mathbf{2_2}$ is an asymmetric Fe hydride dimer with two μ-bridging hydride ligands, where the Fe1 center is pentacoordinated and the Fe2 center is tetracoordinated. The hydrogen atoms corresponding to the hydride ligands in complex $\mathbf{2_2}$ (H1A and H1B) were located in the electron density map. The modes of coordination of the 5-aryl-2-iminopyrrolyl ligands in complex $\mathbf{2_2}$ are the same as in the previous complexes. The tetracoordinated Fe2 center has the Fe2−N4 and Fe2−N5 bond lengths equal to 1.990(2) Å and 2.025(2) Å, respectively. The Fe2−H1 bond lengths are around 1.55 Å and the τ_4 parameter in complex $\mathbf{2_2}$ is 0.07, revealing a square planar geometry around Fe2. The pentacoordinated Fe1 center has a coordinated pyridine ligand, aside from the 5-aryl-2-iminopyrrolyl and the bridging hydride moieties. In this case, the Fe1−N bond lengths are in the range of 2.059−2.180 Å, slightly longer than in the tetracoordinated Fe2 center. The Fe1−H1 bond lengths are around 1.68−1.69 Å, also longer than that observed for the Fe2 center. The τ_5 parameter in the Fe1 center in complex $\mathbf{2_2}$ is 0.60 (τ_5= 1 for an ideal trigonal bipyramid and τ_5= 0 for an ideal square pyramid[28]), thus revealing to be an intermediate case between trigonal bipyramidal and square pyramidal geometries. The different bond lengths involving the two Fe centers, which are larger in Fe1 than in Fe2, point to different electronic environments.

On the other hand, complex **3** is a Fe(I) complex with a η^6-coordinated toluene molecule in which the Fe1−C33 to C38 bond lengths are quite similar, in the range of 2.060(11)−2.149(10) Å (Δ ≈ 0.089 Å). The Fe1−centroid distance (the centroid being defined as the center of the six-membered aromatic ring formed by atoms C33 to C38) is equal to 1.548(6) Å. The Fe1−N bond lengths are in the range 1.971(7)−1.977(8) Å, where the 5-aryl-2-formiminopyrrolyl ligand exhibits the typical bidentate coordination mode. The Fe1−N bond lengths are shorter than in the analogous Co(I) complex [Co{κ^2*N,N'*-5-(2,4,6-^{i}Pr$_3$-C$_6$H$_2$)-NC$_4$H$_2$-2-C(H)=N(2,6-^{i}Pr$_2$-C$_6$H$_3$)}(η^6-C$_6$H$_5$CH$_3$)] reported by our group.[25] Both the Fe1−N and the Fe1-centroid bond lengths are similar to the crystalographically characterized Fe(I) complexes of the type [LFe(toluene)], where L is a bidentate chelating ligand.[6,29] Complex **3** displays a pseudo-tetrahedral coordination geometry (with τ_4 = 0.74), if one considers the tetrahedron formed by the N1, N2, C33 and C36 atoms bonded to Fe1. The η^6-arene moiety is

View Article Online
DOI: 10.1039/C8CY02319K

virtually perpendicular to the chelation plane (87.46º). The torsions of the 5-aryl and the N2-aryl rings relative to the 2-iminopyrrolyl plane are 83.37º and 81.75º, respectively. Additionally, a DFT geometry optimization has been performed for complex **3** in the high spin electronic state, S = 3/2, its optimized atomic coordinates being presented in the ESI. The theoretical structure of complex **3** compares well with its experimentally determined structure.

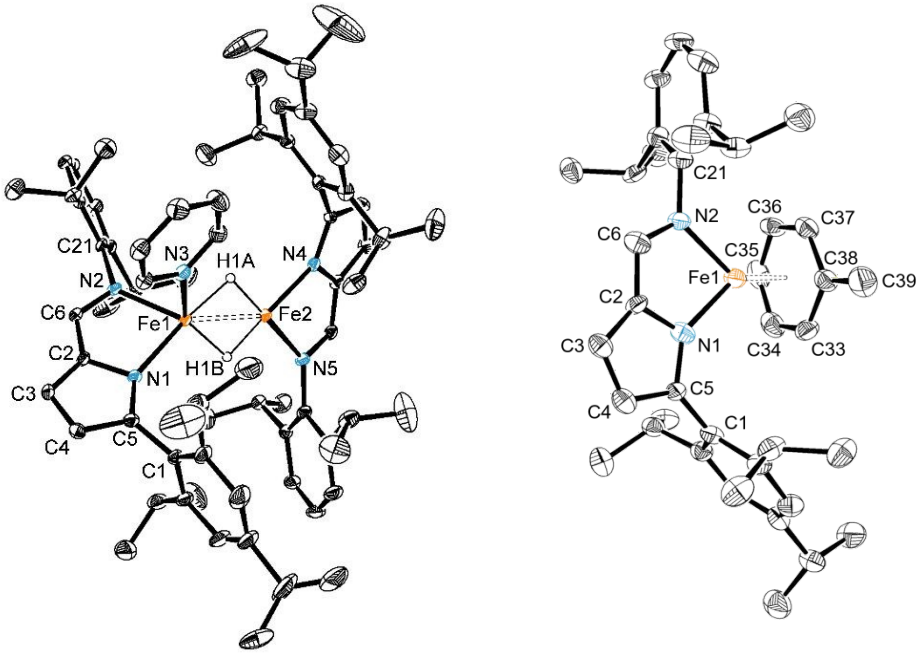

2_2 **3**

Figure 3 ORTEP-3 diagrams for complexes **2_2** and **3** showing 30% probability ellipsoids. All hydrogen atoms except for H1A and H1B were omitted for clarity.

In order to understand the electronic structure of complex **2_2**, geometry optimizations were performed, using DFT calculations. The deviations between calculated and experimental coordination bond lengths of complex **2_2** are presented in Table 4. The geometry optimized for complex **2_2** is similar to the one determined by X-ray diffraction. The calculated Fe–N distances are slightly overestimated (except for Fe2–N5), with a maximum deviation of 4.7%, but the Fe1−N bond lengths are longer than the ones calculate for the Fe2 center, as observed by X-ray diffraction. The larger overestimation (8.2 %) is found for the Fe1−H bond length (average), but still the trend observed in the experimental structure is reproduced, with longer Fe–H distances for the Fe1 center. Those values are reasonable for the level of theory employed that is constrained by the size of the molecule. The τ geometry parameters are also well reproduced in the calculated structure of **2_2**.

View Article Online
DOI: 10.1039/C8CY02319K

Table 4 Comparison of selected bond lengths (in Å) and the appropriate τ geometry parameters in complex $\mathbf{2_2}$ determined by single crystal X-ray diffraction and by DFT calculations.

Parameter	Experimental	Calculated	Δ	Δ (%)
Fe1−N1	2.059(2)	2.14	0.08	3.7
Fe1−N2	2.155(2)	2.26	0.11	4.7
Fe1−N3	2.180(3)	2.23	0.05	2.2
Fe2−N4	1.990(2)	2.01	0.02	1.0
Fe2−N5	2.025(2)	2.01	-0.02	-0.74
Fe1−H1 [a]	1.69(4)	1.84	0.15	8.2
Fe2−H1 [a]	1.55(4)	1.58	0.03	1.9
Fe1−Fe2	2.4874(5)	2.57	0.08	3.2
τ_4	0.07	0.10		
τ_5	0.60	0.69		

[a] The average distance is considered.

The electronic structure of complex $\mathbf{2_2}$ was further studied by a Natural Population Analysis[30] (NPA, see Computational Details) and the results are summarized in Figure 4. The coordination asymmetry of the molecule is reflected in both its electronic structure and spin density. The Wiberg indices[31] involving the Fe1 pentacoordinated center are smaller than the ones observed in the Fe2 tetracoordinated center, indicating weaker Fe1–X bonds, when compared with Fe2–X, in accordance with the bond lengths discussed above. The spin density of the complex is essentially located on the two metal atoms (Figure 4b) but most of it is centered on Fe1 (3.7) with a much lower participation of Fe2 (0.4) where the coordination geometry approaches a square planar arrangement.

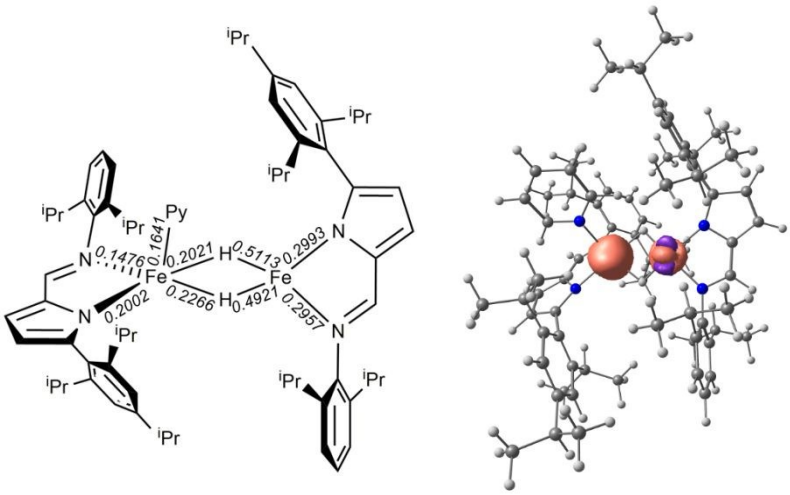

(a) **(b)**

Figure 4 Selected Wiberg indices (a) and calculated spin density (b) in complex $\mathbf{2_2}$.

View Article Online
DOI: 10.1039/C8CY02319K

The isolated mixtures of complexes I and II were further tested in the hydroboration of styrene with HBPin, by reproducing the experimental conditions used in the **1a-d**/K(HBEt$_3$) system. The corresponding set of catalytic experiments performed is summarized in Table 5. In neat conditions, we have observed that the catalytic run using styrene, HBPin and 1 mol% of mixture I (**2** + **2$_2$**) has almost exclusively yielded PinB-BPin (B$_2$Pin$_2$) and a very complex mixture of very minor products, which included the expected mixture of boranes in a *a*-Mk:Mk ratio of 0.37:1 (Figure S28 of the ESI). In light of this somewhat puzzling result, we also performed other control experiments, using only styrene or only HBPin in the catalytic runs, also in neat conditions. We realized that the reaction of mixture I with HBPin also led to the formation of B$_2$Pin$_2$. Catalysis with 1 mol% of mixture II in neat conditions has led to virtually the same *a*-Mk:Mk ratio (0.40:1), with a much higher selectivity towards hydroboration than that obtained with mixture I in neat conditions (Figure S28 of the ESI). Finally, we also performed a catalytic run with mixture I in the presence of a large excess of toluene (4:1 in volume with respect to styrene) and, gratifyingly, observed a much more hydroboration-selective system, with the same *a*-Mk:Mk ratio (0.36:1) (Figure S28 of the ESI).

Table 5 Summary of the catalytic experiments performed with mixtures I and II (see Scheme 2).

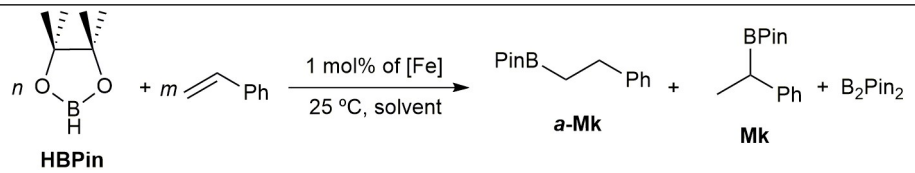

[Fe] catalyst	Amounts[a]	Solvent	Yield[b]	Selectivity (*a*-Mk:Mk:B$_2$Pin$_2$)[c]
Mixture I	n=1; m=0	Neat	44	0:0:1
Mixture I	n=0; m=1	Neat	0	-
Mixture I	n=1; m=1	Neat	52	0.37:1:8.7
Mixture II	n=1; m=1	Neat	41	0.40:1:1.6
Mixture I	n=1; m=1	Toluene	47	0.36:1:1.2
1b/K(HBEt$_3$)	n=1; m=1	Toluene	60	0.37:1:0

[a] Conditions: 1 mol% of mixture I (**2** + **2$_2$**) or 1 mol% of mixture II (**2** + **2$_2$** + **3**) or 1 mol% of **1b** + 3 mol% of K(HBEt$_3$), 2 mmol of styrene, 2.5 mmol of HBPin, reaction time: 16 h, temperature: 25 ºC. [b] Yields determined by weighing the isolated reaction products. [c] Calculated by ^{1}H NMR.

View Article Online
DOI: 10.1039/C8CY02319K

As far as mechanistic considerations for the present system are concerned, we propose this catalyst system follows the oxidative addition pathway represented in Scheme 3.

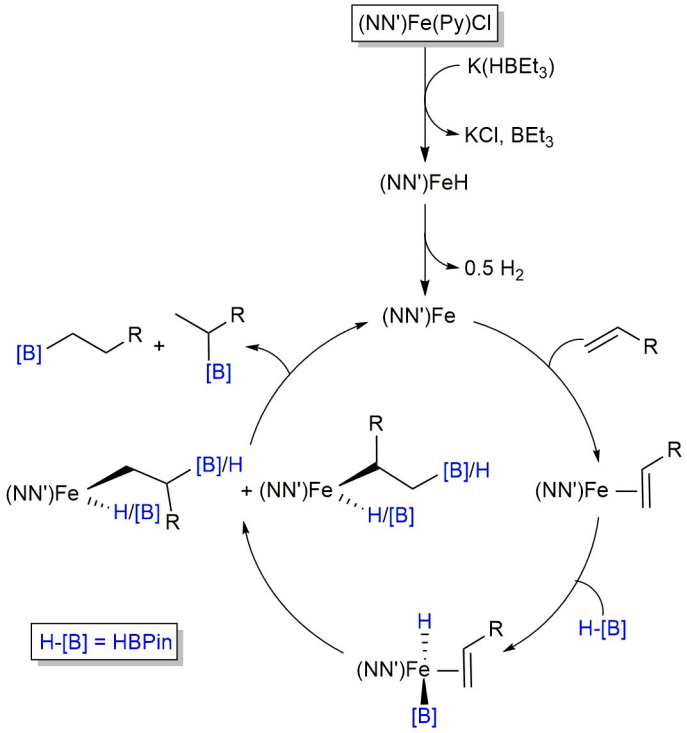

Scheme 3 Proposed catalytic cycle.

Even though the reaction of the pyridine chloride complexes **1a-d** with K(HBEt$_3$) in toluene seems to favor the formation of Fe(II) hydride complexes (*cf.* mixture I of Scheme 2), prolonged stirring in the same solvent leads to an increased concentration of low valent Fe(I) species (*cf.* mixture II of Scheme 2). Furthermore, when testing the catalytic performance of the **2** + **2$_2$** mixture (mixture I, see Scheme 2), we observed that it was virtually non-selective towards hydroboration and such selectivity increased dramatically when the catalytic runs were performed in toluene.

Considering these observations, we propose that in the activation by K(HBEt$_3$), while giving rise to a hydride complex **(NN')Fe$^{(II)}$H**, the coordinative pressure of olefins/arenes during catalysis very likely generates a low oxidation state species "**(NN')Fe$^{(I)}$**" that, by coordination of the respective substrate generates the Fe(I) intermediate **(NN')Fe$^{(I)}$(η^2-CH$_2$=CHR)** (Scheme 3). This Fe(I) entity is prone to oxidative addition of HBPin, possibly giving rise to **(NN')Fe$^{(III)}$(H)(BPin)(η^2-CH$_2$=CHR)**. The resulting hydride-boryl species generates the intermediates **(NN')Fe$^{(III)}$(CH$_2$CHBPinR)(H)** and/or **(NN')Fe$^{(III)}$[CH(R)CH$_2$BPin](H)**, possibly via a migratory insertion of the BPin boryl

moiety. Alternatively, a migratory insertion of the hydride can occur, generating the intermediates **(NN')Fe$^{(III)}$(CH$_2$CH$_2$R)(BPin)** and/or **(NN')Fe$^{(III)}$[CH(R)CH$_3$](BPin)**. Finally, a reductive elimination reaction yields the reaction products and regenerates the active "**(NN')Fe$^{(I)}$**" species. The high Markovnikov selectivity in the case of styrene substrates is very likely justified by a more favorable 2,1-insertion of the boryl or hydride ligands (as opposed to the near quantitative 1,2-insertion in the remaining substrates), thus increasing the amount of the **(NN')Co$^{(III)}$[CH(R)CH$_2$BPin](H)** or **(NN')Co$^{(III)}$[CH(R)CH$_3$](BPin)** intermediate species.

Conclusions

Four new paramagnetic Fe(II) complexes of the type [Fe{κ^2*N,N'*-5-R-NC$_4$H$_2$-2-C(H)=N(2,6-^{i}Pr$_2$-C$_6$H$_3$)}(Py)Cl] (**1a-d**) were prepared via salt metathesis with the respective potassium salts **KLa-d** in moderate yields. The magnetic susceptibilities of complexes **1a-d** were characterized in solution by the Evans method, displaying high-spin electronic configurations. Complexes **1a** and **1c** were characterized by single crystal X-ray diffraction, highlighting distorted tetrahedral geometries. Complex **1a** was additionally characterized in the solid state by SQUID magnetometry and ^{57}Fe Mössbauer spectroscopy, and complexes **1a-d** were studied by DFT calculations, all these techniques reinforcing their high-spin nature.

Complexes **1a-d** are precatalysts for the hydroboration of terminal α-olefins with pinacolborane, when activated by K(HBEt$_3$). The system composed by **1a**/K(HBEt$_3$) was able to hydroborate several terminal alkenes to their respective boronate esters in good yields, mainly yielding the respective *anti*-Markovnikov addition products. However, the screening of the catalytic system **1a-d** /K(HBEt$_3$) with styrene showed that the selectivity in the Markovnikov product increased with the increasing steric bulkiness of the R group, with **1c** (R = 2,4,6-Ph$_3$-C$_6$H$_3$) being 91% selective in the latter product.

The reactivity of complexes **1a-d** with K(HBEt$_3$) was studied, the only isolable product coming from complex **1b**, for which a mixture of Fe(II) hydrides, monomeric species **2** and dimeric **2$_2$**, was obtained (mixture I). Prolonged stirring of **1d** and K(HBEt$_3$) in toluene led to the identification of a third species, identified as the Fe(I) complex **3**, along with **2** + **2$_2$** (mixture II). ^{57}Fe Mössbauer spectroscopy performed on mixtures I and II indicated the presence of three and four different doublets, respectively, a set of two doublets

corresponding to the two-different iron centers in $\mathbf{2_2}$, another doublet corresponding to a Fe(II) high-spin in **2** and, only in mixture II, a further doublet, assigned as the high-spin Fe(I) complex **3**. The DFT calculated structure of complex $\mathbf{2_2}$ shed light on its asymmetry, as both iron centers showed different spin density distributions.

Taking these results into account and considering that the presence of olefinic media is the driving force for the observation of Fe(I) complexes, it is very likely that the present catalytic process follows a route involving the borane oxidative addition to a Fe(I) species.

Experimental

General considerations: All operations were performed under dry dinitrogen atmosphere using standard glovebox and Schlenk techniques unless otherwise stated. Solvents were pre-dried with activated 4 Å molecular sieves and distilled by refluxing under dinitrogen for several hours over suitable drying agents (sodium/benzophenone for diethyl ether, THF and toluene; CaH_2 for *n*-hexane). The substrates used in the catalytic runs were dried over CaH_2 and purified by trap-to-trap distillation. Solvents and solutions were transferred using a positive pressure of dinitrogen through stainless steel cannulae and mixtures were filtered in a similar way using modified cannulae that could be fitted with glass fiber filter disks. $K(HBEt_3)$ was purchased in THF solutions and was used as a solid by recrystallization from the same solvent, being stored at 4 ºC. Pinacolborane was purified by trap-to-trap distillation prior to use. The potassium salts **KLa-d**[17] and $FeCl_2(Py)_4$[32] were prepared as described in the literature. All other reagents were acquired commercially and used without further purification. FTIR measurements were conducted on a Bruker Alpha II ATR IR spectrometer located inside a glovebox. Elemental analyses were obtained from the IST elemental analysis services.

General method for the synthesis of [Fe{κ²*N*,*N'*-5-R-NC$_4$H$_2$-2-C(H)=N(2,6-^{i}Pr$_2$-C$_6$H$_3$)}(Py)Cl] (complexes 1a-d): Toluene was added to a solid mixture of $FeCl_2(Py)_4$ and the respective potassium salt **KLa-d**, at room temperature. The mixture was stirred overnight at 80 ºC, leaving an orange-red suspension. All volatiles were evaporated to dryness, leaving an orange-red residue. The residue was washed with *n*-hexane and extracted with toluene. The combined orange-red extracts were concentrated, carefully layered with *n*-hexane (1:3) and stored at -20 ºC, precipitating the title complexes as orange-red powders or crystals.

View Article Online
DOI: 10.1039/C8CY02319K

[Fe{κ²*N*,*N*'-5-(2,6-Me$_2$-C$_6$H$_3$)-NC$_4$H$_2$-2-C(H)=N(2,6-^{i}Pr$_2$-C$_6$H$_3$)}(Py)Cl] (1a): The general procedure was followed, using 0.32 g (0.8 mmol) of the potassium salt **KLa** and 0.39 g (0.8 mmol) of $FeCl_2(Py)_4$, yielding an orange-red crystalline solid. Yield: 0.21 g (49 %).
Anal. Calc. for $C_{30}H_{34}ClFeN_3$, obtained (calculated): C 68.65 (68.25), H 6.69 (6.49), N 7.65 (7.96). μ_{eff} (toluene-d_8) = 5.3 μ_B. ^{1}H NMR (300 MHz, C_6D_6): δ 50.14, 5.32, 2.11, 1.19, 0.24, -2.30, -12.11, -22.68. FTIR (ATR, cm^{-1}) = 1561 (s, C=N).

[Fe{κ²*N*,*N*'-5-(2,4,6-^{i}Pr$_3$-C$_6$H$_2$)-NC$_4$H$_2$-2-C(H)=N(2,6-^{i}Pr$_2$-C$_6$H$_3$)}(Py)Cl] (1b): The general procedure was followed, using 0.37 g (0.75 mmol) of the potassium salt **KLb** and 0.37 g (0.75 mmol) of $FeCl_2(Py)_4$, yielding an orange-red powder. Yield: 0.117 g (25 %).
Anal. Calc. for $C_{37}H_{48}ClFeN_3$, obtained (calculated): C 70.89 (70.98), H 8.04 (7.73), N 6.32 (6.71). μ_{eff} (toluene-d_8) = 4.8 μ_B. ^{1}H NMR (300 MHz, C_6D_6) δ 70.18, 38.79, 10.27, 3.07, 1.24, -0.72, -1.40, -1.85, -2.29, -4.76, -7.87, -9.36, -19.71. FTIR (ATR, cm^{-1}) = 1565 (s, C=N).

[Fe{κ²*N*,*N*'-5-(2,4,6-Ph$_3$-C$_6$H$_2$)-NC$_4$H$_2$-2-C(H)=N(2,6-^{i}Pr$_2$-C$_6$H$_3$)}(Py)Cl] (1c): The general procedure was followed, using 0.43 g (0.72 mmol) of the potassium salt **KLc** and 0.35 g (0.72 mmol) of $FeCl_2(Py)_4$, yielding an orange-red crystalline solid. Yield: 0.13 g (25 %).
Anal. Calc. for $C_{46}H_{42}ClFeN_3$, obtained (calculated): C 75.51 (75.88), H 5.93 (5.81), N 5.60 (5.77). μ_{eff} (toluene-d_8) = 4.6 μ_B. ^{1}H NMR (300 MHz, C_6D_6) δ 71.28, 36.86, 16.00, 11.33, 8.56, 6.06, 3.74, 2.11, 1.11, -0.07, -3.63, -11.24, -19.78. FTIR (ATR, cm^{-1}) = 1563 (s, C=N).

[Fe{κ²*N*,*N*'-5-(triphenylmethyl)-NC$_4$H$_2$-2-C(H)=N(2,6-^{i}Pr$_2$-C$_6$H$_3$)}(Py)Cl] (1d): The general procedure was followed, using 0.53 g (1 mmol) of the potassium **KLd** and 0.49 g (1 mmol) of $FeCl_2(Py)_4$, yielding an orange-red powder. Yield: 0.16 g (24 %).
Anal. Calc. for $C_{41}H_{40}ClFeN_3$, obtained (calculated): C 73.56 (73.93), H 6.29 (6.05), N 5.92 (6.31). μ_{eff} (toluene-d_8) = 4.7 μ_B. ^{1}H NMR (300 MHz, $CDCl_3$) δ 69.23, 38.91, 21.93, 18.59, 10.77, 9.15, 7.27, 4.33, 3.03, -0.53, -3.02, -13.95. FTIR (ATR, cm^{-1}) = 1573 (s, C=N).

General procedure for catalytic hydroboration reactions: A Schlenk flask was charged with the desired amount of complex **1a-d** (1% mol) and K(HBEt$_3$) (3% mol), after which a solution of the appropriate substrate (2 mmol) and pinacolborane (2.5 mmol) was added. The mixture was stirred at 25 ºC for 16 h and quenched by adding *ca.* 15 mL of *n*-hexane and

View Article Online
DOI: 10.1039/C8CY02319K

exposing the mixture to air. The solution was filtered through a plug of silica and the solvent evaporated to dryness. The resulting pale-yellow oil was eluted with *n*-hexane through a Pasteur pipette mounted with silica. The hydroboration products were isolated as near colorless oils. The selectivity of the products was determined by ^{1}H NMR and their yields were determined by weighing the isolated reaction products.

Isolation of mixture I (2 + 2$_2$): Toluene was added to a solid mixture of complex **1b** (0.30 g, 0.49 mmol) and K(HBEt$_3$) (0.072 g, 0.54 mmol) at room temperature, to give a dark red-brown solution. The mixture was stirred at room temperature for 30 min, to yield a dark red-brown suspension. All volatile materials were evaporated under reduced pressure, to give an oily dark red-brown residue. The residue was redissolved in *n*-hexane with separation of a pale precipitate and a negligible dark residue. The dark red-brown solution was concentrated and stored at -20 ºC, giving rise to a dark red-brown crystalline solid suitable for X-ray diffraction. Yield: 44 % (0.12 g).
Anal. Calc. for $(C_{37}H_{49}FeN_3)_{0.35}(C_{69}H_{93}Fe_2N_5)_{0.65}$ obtained (calculated): C 75.12 (75.07), H 8.50 (8.46), N 6.45 (6.51). μ_{eff} (toluene-d_8) = 4.9 μ_B, considering the formula $(C_{37}H_{49}FeN_3)_{0.35}(C_{69}H_{93}Fe_2N_5)_{0.65}$.

Isolation of mixture II (2 + 2$_2$ + 3): Toluene was added to a solid mixture of complex **1b** (0.30 g, 0.49 mmol) and K(HBEt$_3$) (0.072 g, 0.54 mmol) at room temperature, to give a dark red-brown solution. The mixture was stirred at room temperature for 16 h, to yield a dark red-brown suspension. All volatile materials were evaporated under reduced pressure, to give an oily dark red-brown residue. The residue was redissolved in *n*-hexane with separation of a pale precipitate and a negligible dark residue. The dark red-brown solution was concentrated and stored at -20 ºC, giving rise to a dark red-brown crystalline solid suitable for X-ray diffraction. Yield: 55 % (0.15 g).
Anal. Calc. for $(C_{37}H_{49}FeN_3)_{0.34}(C_{69}H_{93}Fe_2N_5)_{0.56}(C_{39}H_{51}FeN_2)_{0.1}(\text{-Osi}(CH_3)_2\text{-})_{0.5}$ obtained (calculated): C 72.93 (73.48), H 8.47 (8.45), N 6.05 (6.14). μ_{eff} (toluene-d_8) = 5.0 μ_B, considering the formula $(C_{37}H_{49}FeN_3)_{0.34}(C_{69}H_{93}Fe_2N_5)_{0.56}(C_{39}H_{51}FeN_2)_{0.1}(OSiMe_2)_{0.5}$.

NMR measurements: NMR spectra were recorded on a *Bruker "AVANCE III"* 300 MHz, at 299.995 MHz (^{1}H), and referenced internally using the residual protio-resonances of the corresponding solvents to tetramethysilane (δ = 0). Deuterated solvents were dried over

activated 4 Å molecular sieves and degassed by the freeze-pump-thaw technique, and stored under dinitrogen in J. Young ampoules.

Magnetic susceptibility measurements in solution were carried out using the Evans method,[19] using a 3% solution of hexamethyldisiloxane in toluene-d_8. These solutions were prepared in a glovebox in J. Young NMR tubes containing capillary tubes filled with the same solvent mixture, in which the hexamethyldisiloxane is the external reference.

X-ray diffraction: Crystallographic and experimental details of crystal structure determinations are listed in Table S1 of the ESI. The crystals were selected under dinitrogen, covered with polyfluoroether oil and mounted on a nylon loop. Crystallographic data were collected using graphite monochromated Mo-Kα radiation (λ = 0.71073 Å) on a Bruker AXS-KAPPA APEX II diffractometer equipped with an Oxford Cryosystem open-flow nitrogen cryostat, at 150 K. Cell parameters were retrieved using Bruker SMART[33] software and refined using Bruker SAINT[34] on all observed reflections. Absorption corrections were applied using SADABS.[35] Structure solution and refinement were performed using direct methods with the programs SIR2014[36] and SHELXL[37] included in the package of programs WINGX-Version 2014.1.[38] Crystals of complex **1c** were of poor quality, presenting a relatively low ratio of observed/unique reflections. Though the structure of complex **1c** was refined to a perfect convergence, it is only presented in Figure S6 of the ESI as a proof of its connectivity. All hydrogen atoms were inserted in idealized positions and allowed to refine riding on the parent carbon atom, except for the hydride hydrogen atoms H1A and H1B of complex 2_2, which were located on the electron density map. All the structures refined to a perfect convergence. Graphic presentations were prepared with ORTEP-3.[38b,39] Data was deposited in CCDC under the deposit numbers 1875120 for **1a**, 1875121 for **1c**, 1875122 for $\mathbf{2_2}$ and 1908799 for **3**.

Solid state magnetic measurements: The magnetic properties of complex **1a** were studied using a 6.5 T *S700X SQUID* (Cryogenic Ltd.) magnetometer. The magnetic susceptibility was measured as a function of temperature in increasing temperature range 5-300 K using a DC magnetic field of 500 Oe. The paramagnetic data was obtained after the correction for the core diamagnetism estimated using Pascal's constants, giving χ_D= -370.2×10^{-6} emu/mol.

Mössbauer spectroscopy: Mössbauer spectra for complexes **1a** and the mixtures I and II of Fe complexes were collected between 295 and 4 K in transmission mode using a conventional constant-acceleration spectrometer and a 25 mCi ^{57}Co source in a Rh matrix. The velocity scale was calibrated using α-Fe foil. Isomer shifts, IS, are given relative to this standard at room temperature. The absorbers were obtained by gently packing the powdered samples (5 mg of natural Fe cm^{-2}) into Perspex holders. Low-temperature measurements were performed with the sample immersed in liquid He in a bath cryostat for measurements at 4.1 K and in He exchange gas in the same cryostat for temperatures higher than 4.1 K. The spectra were fitted to Lorentzian lines using a non-linear least-squares method.[40]

Computational details: All calculations were performed using the Gaussian 09 software package[41] and the OPBE functional. OPBE combines the Handy's OPTX modification of Becke's exchange functional[42] and the gradient-corrected correlation functional of Perdew, Burke and Ernzerhof,[43] and was shown to be accurate in the calculation of spin state energy splitting for first transition row species.[44] The geometry optimizations were accomplished without symmetry constraints using a standard 6-31G** basis set[45] for all atoms except for iron, that used the LanL2DZ[46] (for complexes **1a-d** and **3**) or Effective Core Potential SDD[47] (for complexes **2** and $\mathbf{2_2}$) basis set with a *f*-polarization function for Fe.[48] A Natural Population Analysis (NPA)[30] and the resulting Wiberg indices[31] were used to study the electronic structure and bonding of the optimized species. The spin density plot of $\mathbf{2_2}$ was represented using ChemCraft.[49]

Acknowledgements

We thank Fundação para a Ciência e a Tecnologia for the financial support (Projects UID/QUI/00100/2019 and UID/Multi/04349/2019) and the fellowships to T.F.C.C. and P.T.G. (PD/BD/52372/2013 – CATSUS PhD Program and SFRH/BSAB/140115/2018, respectively).

References

1 V. P. Ananikov, M. Tanaka, *Hydrofunctionalization*, Vol. 43, Springer, 2013.

2 For example: (a) S. A. Westcott, H. P. Blom, T. B. Marder, R. T. Baker, *J. Am. Chem. Soc.*, 1992, **114**, 8863−8869; (b) K. Burgess, W. A. van der Donk, S. A. Westcott, T. B.

View Article Online
DOI: 10.1039/C8CY02319K

Marder, R. T. Baker, J. C. Calabrese, *J. Am. Chem. Soc.*, 1992, **114**, 9350−9359; (c) S. A. Westcott, T. B. Marder, R. T. Baker, *Organometallics*, 1993, **12**, 975−979; (d) C. M. Vogels, S. A. Westcott, *Curr. Org. Chem.*, 2005, **9**, 687−699; (e) K. Burgess, M. J. Ohlmeyer, *Chem. Rev.*, 1991, **91**, 1179–1191; (f) C. M. Crudden, D. Edwards, *Eur. J. Org. Chem.*, 2003, 4695–4712; (g) S. P. Thomas, V. K. Aggarwal, *Angew. Chem. Int. Ed.*, 2009, **48**, 1896–1898.

3 R. M. Bullock, *Catalysis without Precious Metals*; Wiley-VCH: Weinheim, 2010.

4 For example: (a) J. V. Obligacion, P. J. Chirik, *Org. Lett.*, 2013, **15**, 2680–2683; (b) J. V. Obligacion, P. J. Chirik, *J. Am. Chem. Soc.*, 2013, **135**, 19107−19110; (c) W. N. Palmer, T. Diao, I. Pappas, P. J. Chirik, *ACS Catal.*, 2015, **5**, 622–626; (d) M. L. Scheuermann, E. J. Johnson, P. J. Chirik, *Org. Lett.*, 2015, **17**, 2716–2719; (e) A. J. Ruddy, O. L. Sydora, B. L. Small, M. Stradiotto, L. Turculet, *Chem. Eur. J.*, 2014, **20**, 13918–13922; (f) H. Zhang, Z. Lu, *ACS Catal.*, 2016, **6**, 6596–6600; (g) A. J. MacNair, C. R. P. Millet, G. S. Nichol, A. Ironmonger, S. P. Thomas, *ACS Catal.*, 2016, **6**, 7217–7221; (h) J. Y. Wu, B. Moreau, T. Ritter, *J. Am. Chem. Soc.*, 2009, **131**, 12915–12917; (i) L. Zhang, Z. Zuo, X. Leng, Z. Huang, *Angew. Chem. Int. Ed.*, 2014, **53**, 2696–2700; (j) M. Espinal-Viguri, C. R. Woof, R. L. Webster, *Chem. Eur. J.*, 2016, **33**, 11605–11608; (k) K.-N. T. Tseng, J. W. Kampf, N. K. Szymczak, *ACS Catal.*, 2015, **5**, 411–415; (l) Z. Chen, Z. Cheng, Z. Lu, *Org. Lett.*, 2017, **19**, 969–971; (m) T. Ogawa, A. J. Ruddy, O. L. Sydora, M. Stradiotto, L. Turculet, *Organometallics*, 2017, **36**, 417–423; (n) J. Peng, J. H. Docherty, A. P. Dominey, S. P.; Thomas, *Chem. Commun.*, 2017, **53**, 4726−4729; (o) Z. Zuo, J. Yang, Z. Huang, *Angew. Chem. Int. Ed.*, 2017, **55**, 10839−10843; (p) G. Zhang, J. Wu, M. Wang, H. Zeng, J. Cheng, M. C. Neary, S. Zheng, *Eur. J. Org. Chem.*, 2017, **38**, 5814−5818.

5 (a) J. M. Smith, R. J. Lachicotte, P. L. Holland, *Chem. Comm.*, 2001, 1542–1543. (b) J. M. Smith, R. J. Lachicotte, P. L. Holland, *Organometallics*, 2002, **21**, 4808. (c) R. E. Cowley, P. L. Holland, *Inorg. Chem.*, 2012, **51**, 8352−8361. (d) M. M. Rodriguez, E. Bill, W. W. Brennessel, P. L. Holland, *Science*, 2011, **334**, 780.

6 R. P. Rose, C. Jones, C. Schulten, S. Aldridge, A. Stasch, *Chem. Eur. J.*, 2008, **14**, 8477–8480.

7 E. R. King, T. A. Betley, *Inorg. Chem.*, 2009, **48**, 2361–2363; (b) E. R. King, E. T. Hennessy, T. A. Betley, *J. Am. Chem. Soc.*, 2011, **133**, 4917–4923.

View Article Online
DOI: 10.1039/C8CY02319K

8 D. M. Dawson, D. A. Walker, M. Thornton-Pett, M. Bochmann, *J. Chem. Soc. Dalton Trans.*, 2000, 459–466.

9 G. Jiao, G. Zhu, S. Zhang, H. Sun, *Z. Anorg. Allg. Chem.*, 2015, **11**, 1959–1963.

10 (a) S. A. Carabineiro, R. M. Bellabarba, P. T. Gomes, S. I. Pascu, L. F. Veiros, C. Freire, L. C. J. Pereira, R. T. Henriques, M. C. Oliveira, J. E. Warren, *Inorg. Chem.*, 2008, **47**, 8896–8911. (b) S. A. Carabineiro, L. C. Silva, P. T. Gomes, L. C. J. Pereira, L. F. Veiros, S. I. Pascu, M. T. Duarte, R. T. Henriques, *Inorg. Chem.*, 2007, **46**, 6880–6890. (c) C. S. B. Gomes, S. A. Carabineiro, P. T. Gomes, M. T. Duarte, M. A. N. D. A. Lemos, *Inorg. Chim. Acta*, 2011, **367**, 151–157.

11 C. S. B. Gomes, M. T. Duarte, P. T. Gomes, *J. Organomet. Chem.*, 2014, **760**, 167–176.

12 C. S. B. Gomes, P. T. Gomes, M. T. Duarte, R. E. Di Paolo, A. L. Maçanita, M. J. Calhorda, *Inorg. Chem.*, 2009, **48**, 11176–11186.

13 C. S. B. Gomes, D. Suresh, P. T. Gomes, L. F. Veiros, M. T. Duarte, T. G. Nunes, M. C. Oliveira, *Dalton Trans.*, 2010, **39**, 736–748.

14 (a) D. Suresh, C. S. B. Gomes, P. T. Gomes, R. E. Di Paolo, A. L. Maçanita, M. J. Calhorda, A. Charas, J. Morgado, M. T. Duarte, M. T. *Dalton Trans.*, 2012, **41**, 8502–8505; (b) M. J. Calhorda, D. Suresh, P. T. Gomes, R. E. Di Paolo, A. L. Maçanita, *Dalton Trans.*, 2012, **41**, 13210–13217; (c) P. T. Gomes, D. Suresh, C. S. B. Gomes, P. S. Lopes, C. A. Figueira, World Patent WO2013039413, 2013; (d) D. Suresh, P. S. Lopes, B. Ferreira, C. A. Figueira, C. S. B. Gomes, P. T. Gomes, R. E. Di Paolo, A. L. Maçanita, M. T. Duarte, A. Charas, J. Morgado, M. J. Calhorda, *Chem. Eur. J.*, 2014, **20**, 4126–4140; (e) D. Suresh, P. T. Gomes, *Advances in Organometallic Chamistry and Catalysis*, Chapter 36, Wiley, 2013; (f) D. Suresh, C. S. B. Gomes, P. S. Lopes, C. A. Figueira, B. Ferreira, P. T. Gomes, R. E. Di Paolo, A. L. Maçanita, M. T. Duarte, A. Charas, J. Morgado, D. Vila-Viçosa, M. J. Calhorda, *Chem. Eur. J.*, 2015, **21**, 9133–9149; (g) D. Suresh, B. Ferreira, P. S. Lopes, C. S. B. Gomes, P. Krishnamoorthy, A. Charas, D. Vila-Viçosa, J. Morgado, M. J. Calhorda, A. L. Maçanita, P. T. Gomes, *Dalton Trans.*, 2016, **45**, 15603–15620.

15 (a) C. A. Figueira, P. S. Lopes, P. T. Gomes, *Tetrahedron*, 2015, **71**, 4362–4371; (b) C. A. Figueira, P. S. Lopes, C. S. B. Gomes, L. F. Veiros, P. T. Gomes, *CrystEngComm*, 2015, **17**, 6406–6419.

View Article Online
DOI: 10.1039/C8CY02319K

16 T. F. C. Cruz, C. A. Figueira, J. C. Waerenborgh, L. C. J. Pereira, P. T. Gomes, *Polyhedron* 2018, **152**, 179–187.

17 T. F. C. Cruz, P. S. Lopes, L. C. J. Pereira, L. F. Veiros, P. T. Gomes *Inorg. Chem.* 2018, **57**, 8146–8159.

18 (a) C. A. Figueira, P. S. Lopes, C. S. B. Gomes, J. C. S. Gomes, F. Lemos, P. T. Gomes, *Dalton Trans.*, 2018, **47**, 15857–15872; (b) C. A. Figueira, P. S. Lopes, C. S. B. Gomes, J. C. S. Gomes, L. F. Veiros, F. Lemos, P. T. Gomes, *Organometallics*, 2019, **38**, 614–625.

19 (a) D. F. Evans, *J. Chem. Soc.*, 1959, 2003–2005; (b) S. K. Sur, *J. Magnet. Res.*, 1989, **82**, 169–173.

20 (a) F. A. Cotton, G. Wilkinson, C. A. Murillo, M. Bochmann, *Advanced Inorganic Chemistry*; 6th ed., Wiley, 1999; (b) N. N. Greenwood A. Earnshaw, Chemistry of the Elements, 2nd ed., Elsevier Butterworth-Heinemann, 1997.

21 L. Yang, D. B. Powell and R. P. Houser, *Dalton Trans.*, 2007, 955−964.

22 R. G. Parr, W. Yang, *Density Functional Theory of Atoms and Molecules*, Oxford University Press, New York, 1989.

23 N. N. Greenwood, T. C. Gibb, *Mössbauer Spectroscopy*, Chapman and Hall, Ltd. Publishers, London, 1971.

24 P. Gütlich, R. Link, A. Trautwein, *Mössbauer Spectroscopy and Transition Metal Chemistry*, Springer-Verlag, Berlin, Heidelberg, 1978.

25 T. F. C. Cruz, L. F. Veiros, P. T. Gomes, *Inorg. Chem.* 2018, **57**, 14671–14685.

26 (a) T. R. Dugan, E. Bill, K. C. MacLeod, W. W. Brennessel, P. L. Holland, *Inorg. Chem.*, 2014, **53**, 2370–2380; (b) A. Kochem, E. Bill, F. Neese, M. van Gastel, M. *Chem. Commun.*, **2015**, *59,* 2099.

27 (a) E. Bill, *Nat. Chem.* 2013, **5**, 556–557; (b) H. Lee, M. G. Campbell, R. H. Sánchez, J. Börgel, J. Raynaud, S. E. Parker, T. Ritter, *Organometallics*, 2016, **35**, 2923–2929.

28 (a) A. W. Addison, T. N. Rao, J. Reedijk, J. van Rijn, G. G. Verschoor, *J. Chem. Soc., Dalton Trans.*, 1984, 1349-1356; (b) C. O'Sullivan, G. Murphy, B. Murphy, B. J. Hathaway, *J. Chem. Soc., Dalton Trans.* 1999, 1835–1844.

29 (a) S. Yao, T. Szilvási, N. Lindenmaier, Y. Xiong, S. Inoue, M. Adelhardt, J. Sutter, K. Meyerc, M. Driess, *Chem. Commun.*, 2015, **51**, 6153–6156; (b) F. Spitzer, C. Graßl, G. Balázs, E. M. Zolnhofer, K. Meyer, M. Scheer, *Angew. Chem. Int. Ed.*, 2016, **55**, 4340–4344; (c) S. Zlatogorskya, M. J. Ingleson, *Dalton Trans.*, 2012, **41**, 2685–2693.

View Article Online
DOI: 10.1039/C8CY02319K

30 (a) J. E. Carpenter, F. Weinhold, *J. Mol. Struct. (Theochem)*, 1988, **169**, 41; (b) J. E. Carpenter, *PhD thesis*, University of Wisconsin (Madison WI), 1987. (c) J. P. Foster, F. Weinhold, *J. Am. Chem. Soc.*, 1980, **102**, 7211; (d) A. E. Reed, F. Weinhold, *J. Chem. Phys.*, 1983, **78**, 4066; (e) A. E. Reed, F. Weinhold, *J. Chem. Phys.*, 1983, **78**, 1736; (f) A. E. Reed, R. B. Weinstock, F. Weinhold, *J. Chem. Phys.*, 1985, **83**, 735; (g) A. E. Reed, L. A. Curtiss, F. Weinhold, *Chem. Rev.*, 1988, **88**, 899–926; (h) F. Weinhold, J. E. Carpenter, *The Structure of Small Molecules and Ions*, Plenum, 1988, p. 227.

31 (a) K. B. Wiberg, *Tetrahedron*, 1968, **24**, 1083–1096. (b) Wiberg indices are electronic parameters related with the electron density in between two atoms, which scale as bond strength indicators. They can be obtained from a Natural Population Analysis.

32 H. S. Booth, *Inorganic Syntheses*, Vol. 1, McGraw-Hill, 184–185, 1939.

33 SMART Software for the CCD Detector System Version 5.625, Bruker AXS Inc., Madison, WI, USA, 2001.

34 SAINT Software for the CCD Detector System, Version 7.03, Bruker AXS Inc., Madison, WI, USA, 2004.

35 G. M. Sheldrick, SADABS, Program for Empirical Absorption Correction, University of Göttingen, Göttingen, 1996.

36 M. C. Burla, R. Caliandro, B. Carrozzini, G. L. Cascarano, C. Cuocci, C. Giacovazzo, M. Mallamo, A. Mazzone, G. Polidori, *J. Appl. Cryst.*, 2015, **48**, 306.

37 (a) SHELXL: G. M. Sheldrick, *Acta Crystallogr. Sect. C: Struct. Chem.*, 2015, **71**, 3–8; (b) C. B. Hübschle, G. M. Sheldrick, B. Dittrich, *J. Appl. Crystallogr.*, 2011, **44**, 1281–1284.

38 (a) L. J. Farrugia, *J. Appl. Crystallogr.*, 1999, **32**, 837–838; (b) L. J. Farrugia, *J. Appl. Crystallogr.*, 2012, **45**, 849–854.

39 (a) M. N. Burnett, C. K. Johnson, ORTEP-III: Oak Ridge Thermal Ellipsoid Plot Program for Crystal Structure Illustration, Oak Ridge National Laboratory, 1996. Report ORNL-6895; (b) ORTEP-3 for Windows: L. J. Farrugia, *J. Appl. Crystallogr.*, 1997, **30**, 565.

40 J. C. Waerenborgh, P. Salamakha, O. Sologub, A. P. Gonçalves, C. Cardoso, S. Sério, M. Godinho, M. Almeida, *Chem. Mater.*, 2000, **12**, 1743–1749.

41 Gaussian 09, Revision A.01, M. J. Frisch, G. W. Trucks, H. B. Schlegel, G. E. Scuseria, M. A. Robb, J. R. Cheeseman, G. Scalmani, V. Barone, B. Mennucci, G. A. Petersson, H. Nakatsuji, M. Caricato, X. Li, H. P. Hratchian, A. F. Izmaylov, J. Bloino, G. Zheng,

View Article Online
DOI: 10.1039/C8CY02319K

J. L. Sonnenberg, M. Hada, M. Ehara, K. Toyota, R. Fukuda, J. Hasegawa, M. Ishida, T. Nakajima, Y. Honda, O. Kitao, H. Nakai, T. Vreven, J. A. Montgomery Jr., J. E. Peralta, F. Ogliaro, M. Bearpark, J. J. Heyd, E. Brothers, K. N. Kudin, V. N. Staroverov, R. Kobayashi, J Normand, K. Raghavachari, A. Rendell, J. C. Burant, S. S. Iyengar, J. Tomasi, M. Cossi, N. Rega, J. M. Millam, M. Klene, J. E. Knox, J. B. Cross, V. Bakken, C. Adamo, J. Jaramillo, R. Gomperts, R. E. Stratmann, O. Yazyev, A. J. Austin, R. Cammi, C. Pomelli, J. W. Ochterski, R. L. Martin, K. Morokuma, V. G. Zakrzewski, G. A. Voth, P. Salvador, J. J. Dannenberg, S. Dapprich, A. D. Daniels, Ö Farkas, J. B. Foresman, J. V. Ortiz, J. Cioslowski, D. J. Fox, Gaussian, Inc., Wallingford CT, 2009.

42 (a) N. C. Handy, A. J. Cohen *Mol. Phys.*, 2001, **99**, 403–412; (b) H.-M. Hoe, A. Cohen, N. C. Handy, *Chem. Phys. Lett.*, 2001, **341**, 319–328.

43 (a) J. P. Perdew, K. Burke, M. Ernzerhof, *Phys. Rev. Lett.*, 1996, **77**, 3865–3868; (b) J. P. Perdew, K. Burke, M. Ernzerhof, *Phys. Rev. Lett.*, 1997, **78**, 1396.

44 (a) M. Swart *J. Chem. Theory Comput.*, 2008, **4**, 2057–2066; (b) J. Conradie, A. Ghosh, *J. Chem. Theory Comput.*, 2007, **3**, 689–702; (c) J. Conradie, A. Ghosh, *J. Phys. Chem. B*, 2007, **111**, 12621–12624.

45 (a) A. D. McLean, G. S. Chandler, *J. Chem. Phys.*, 1980, **72**, 5639–5648; (b) R. Krishnan, J. S. Binkley, R. Seeger, J. A. Pople, *J. Chem. Phys.*, 1980, **72**, 650–654; (c) A. J. H. Wachters, *J. Chem. Phys.*, 1970, **52**, 1033; (d) P. J. Hay, *J. Chem. Phys.*, 1977, **66**, 4377–4384; (e) K. Raghavachari, G. W. Trucks, *J. Chem. Phys.*, 1989, **91**, 1062–1089; (f) R. C. Binning, L. A. Curtiss, *J. Comput. Chem.*, 1995, **103**, 6104; (g) M. P. McGrath, L. Radom, *J. Chem. Phys.*, 1991, **94**, 511–516.

46 (a) T. H. Dunning Jr., P. J. Hay, *Modern Theoretical Chemistry*, Ed. Schaefer, H.F. III (Plenum, New York, 1976), vol. 3, p. 1; (b) P. J. Hay, W. R. Wadt, *J. Chem. Phys.*, 1985, **82**, 270; (c) W. R. Wadt, P. J. Hay, *J. Chem. Phys.*, 1985, **82**, 284. (d) P. J. Hay, W. R. Wadt, *J. Chem. Phys.*, 1985, **82**, 2299.

47 (a) P. Fuentealba, H. Stoll, L. V. Szentpály, P. Schwerdtfeger, H. Preuss, *J. Phys. B*, 1983, **16**, 323–328; (b) U. Wedig, M. Dolg, H. Stoll, H. Preuss, *Quantum Chemistry: The Challenge of Transition Metals and Coordination Chemistry*, Ed. A. Veillard, Reidel, and Dordrecht, 1986; (c) M. Dolg, U. Wedig, H. Stoll, H. Preuss, *J. Chem. Phys.*, 1987, **86**, 866–872.

View Article Online
DOI: 10.1039/C8CY02319K

48 A. W. Ehlers, M. Böhme, S. Dapprich, A. Gobbi, A. Höllwarth, V. Jonas, K. F. Köhler, R. Stegmann, A. Veldkamp, G. Frenking, *Chem. Phys. Lett.*, 1993, **208**, 111.

49 https://www.chemcraftprog.com.